Emergence, Exploration and Learning of Embodied Behavior

Yasuo Kuniyoshi[1], Shinsuke Suzuki[1], and Shinji Sangawa[1]

Laboratory for Intelligent Systems and Informatics, Department of Mechano-Informatics, School of Information Science and Technology, The University of Tokyo, Tokyo, Japan kuniyosh@isi.imi.i.u-tokyo.ac.jp

1 Introduction

The real world is full of unexpected changes, contingencies and opportunities. Thus it is virtually impossible to perfectly specify in advance all the conditions, states and outcomes for all the possible actions. The so-called "frame problem" was originally discovered with symbolic reasoning agents [6], but essentially it affects any "intelligent" system that relies on explicit descriptions about the states and actions. For example, in control theory terms, the target system can abruptly deviate from the assumed model of the system dynamics, making the pre-defined control law invalid.

The above problem shows up in a wide range of robot behavior, particularly when the situation is complex and fluid. Cognitive interactive tasks such as recognizing another agent's behavior and imitating the task or generating helpful/competing responses often involves high unpredictability due to the caprice and complexity of human behavior and the mutual dependency between the agents' behavior. Even at the level of physical motion control, the situation can be highly complex and unpredictable with a complex body such as a humanoid and the characteristics of the dynamics such as non-linearity, under-actuation, contact states, and rough terrain.

Various adaptive methods have been developed in the past with successful robotic experiments. However, they are either too slow to converge or too narrow in terms of the adaptation range. For example, the most popular learning methods such as reinforcement learning and genetic algorithm both require vast number of trials to converge, and when the bodily or environmental condition changes, they need thousands of trials again to adapt. Moreover, these methods require careful design of the state representation which is not always straightforward unless the characteristics of the body and the environment is well understood.

This paper proposes a novel alternative method for motor behavior emergence. Our model assumes no predefined motion primitives nor state representation. It discovers and exploits the natural dynamics of body-environment interaction. It adapts to the dynamic change of the bodily or environmental structures very quickly, in a *few seconds*. It has biological correlates such as spine/medulla circuit and general movements (GM) that play an important role in very early motor development of human babies.

In the following sections, we first review the issue of exploiting natural body-environment dynamics. Then we present our model which facilitates the emergence of behavior exploiting such dynamics, with some experimental results. In the final part we present our ongoing effort on simulating early human motor development based on the model.

2 Exploiting Embodied Dynamical Structures

In dynamic motion control, exploiting the property of natural body-environment dynamics is very important in order to achieve robustness and efficiency. A well-known example of a meaningful behavior based on pure body-environment dynamics is the passive dynamic walker [5]. And one way to successfully exploit and extend the natural dynamics is to combine it with neural oscillators [10]. These and related issues are gaining more and more interests with quickly accumulating knowledge.

Another related example is juggling. It is also a rhythmic and cyclic motion but somewhat simpler than biped walking. Its dynamics is well understood and effective control methods are proposed [8, 1].

Recently, we presented an example of exploiting acyclic dynamics of whole-body humanoid motion called "roll-and-rise" [3]. Our adult-size humanoid robot first lies flat on the floor, then swings up and down both of the legs, rolling on the back and achieving a crouching posture very quickly. The task requires exploitation and switching of multiple body-environment dynamics with different constraints.

The above and other related examples show that very simple controllers can realize very robust and efficient motion if they properly exploit the natural body-environment dynamics. An outstanding question is how to automatically discover the dynamics and exploit it. This can be a very difficult problem if we assume a body with many degrees of freedom and changing constraints.

3 Emergent Coordination of Multiple Degrees of Freedom

We propose a novel model in which a distributed set of chaotic elements are coupled with the multi-element musculo-skeletal system. Consistent motor behavior patterns emerge from embodied interactions. The same principle gives rise to immediate adaptation capability to changing constraints and switching to different/novel motion patterns. It requires no training or evaluation function. The system autonomously explores, discovers, and exploits possible motion patterns.

3.1 Coupled chaotic system

Coupled Map Lattice(CML) and Globally Coupled Map(GCM)[2] have been investigated in complex systems science for their rich dynamics properties. They follow (1)-(2). CML is a coupled chaotic system with local interaction (1). GCM is one with global interaction (2).

$$x_{n+1}^{i} = (1-\varepsilon) f\left(x_{n}^{i}\right) + \frac{\varepsilon}{2}\left\{f\left(x_{n}^{i+1}\right) + f\left(x_{n}^{i-1}\right)\right\} \tag{1}$$

$$x_{n+1}^{i} = (1-\varepsilon) f\left(x_{n}^{i}\right) + \frac{\varepsilon}{N}\sum_{j=1}^{N} f\left(x_{n}^{j}\right) \tag{2}$$

Where, x_n^i denotes the internal state of ith element at time n, N the total number of elements, and ε the connection weight between elements. $f(x)$ can be any chaos function. In this paper, we adopt a standard *logistic map* represented as the following.

$$f(x) = 1 - ax^2 \tag{3}$$

With no interaction between the elements, all of them behave chaotically. But with interaction, depending on the parameters (a, ε), a rich variety of dynamical structures emerge such as ordered phases (with clusters of resonating elements) and partially ordered phases (configuration of the clusters changes with time).

This phenomenon is essentially caused by a competition of two tendencies; (1) A tendency to synchronize each other by the effect of the mean-field, and (2) a tendency to take arbitrarily different values due to the nature of chaos dynamics.

3.2 Body and environment as an interaction field of chaotic elements

Figure 1 shows our model of chaos coupling through robotic embodiment.

N chaotic elements are connected with actuators and sensors of the robot body. Each element drives a corresponding actuator based on its current internal state. The effect of N actuators collectively change the physical state of the body which is constrained by and interacting with the environment. In other words, the output of N chaotic elements are mixed together and transformed by the embodied dynamics. The result is then sensed at each site of the actuator, e.g. in terms of joint angle or muscle length. Each sensor value is then input to the corresponding chaotic element. Then each element updates, by chaotic mapping, its internal state from the new sensor value and the previous internal state.

The important points of our model are as follows :

- A chaotic element connect each sensor and actuator.

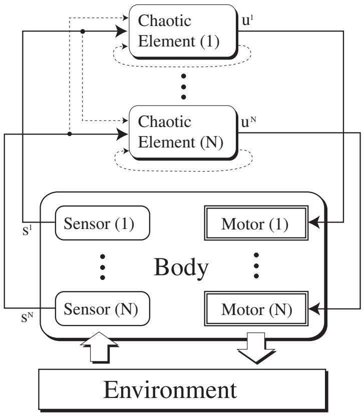

Fig. 1. Outline of our model

- Each actuator is coupled to the body via a spring, simulating a muscle. Each sensor measures the deformation of the spring. Thus, the actuators collectively affect the dynamic state of the body. And the sensors get the mixed effects of the corresponding actuator and the global state of the body.
- The body and the environment interacts. Together, they serve as the interaction field of the chaotic elements.

In our model, body-environment interaction dynamics, or *embodiment*, serves as the chaos coupling field, which is non-linear and time-varying. Theoretically very little is known about such cases, but since the coupling field directly reflects the current body-environment dynamics, we believe that the emergent ordered patterns correspond to useful motor coordination patterns which immediately get reorganized in response to dynamically changing environmental situation.

We devised 3 types of formula to update the internal state of an element : (4), (5), and (6). Where, u denotes the internal state, s the sensor value, and $\bar{s}$ the mean of sensor values. The 2nd and the 3rd terms in f of (4) and (6) are intended to be GCM-like connection and CML-like connection. $\varepsilon_1, \varepsilon_2$ are the weight of each connection. We used logistic map (3) for $f(x)$[1]. Initial condition of u is a random value within $(0, 1)$.

Table 1 shows the interpretation of each formula [2].

[1] In implementation, to avoid divergence, x is constrained as follows : $if(x > 1)\ x = 1,\ if(x < -1)\ x = -1$

[2] In order to understand the “adjustment” effect, the GCM/CML equations should be transformed by applying f on both sides and re-arranged to match (4)-(6)

$$\text{Type-A} \ : \ u_n^i = f\left\{u_{n-1}^i + \varepsilon_1\left(\bar{s}_{n-1} - s_{n-1}^i\right) + \varepsilon_2\left(\frac{s_{n-1}^{i+1} + s_{n-1}^{i-1}}{2} - s_{n-1}^i\right)\right\} \quad (4)$$

$$\text{Type-B} \ : \ u_n^i = f\left(s_n^i\right) \quad (5)$$

$$\text{Type-C} \ : \ u_n^i = f\left\{s_{n-1}^i + \varepsilon_1\left(\bar{s}_{n-1} - s_{n-1}^i\right) + \varepsilon_2\left(\frac{s_{n-1}^{i+1} + s_{n-1}^{i-1}}{2} - s_{n-1}^i\right)\right\} \quad (6)$$

Table 1. Interpretation of the update rules of the coupled chaotic systems

GCM	Each element follows its own pure chaos dynamics with some adjustment to approach the global mean value of all the other pure chaos elements.
CML	Each element follows its own pure chaos dynamics with some adjustment to approach the local mean value of the adjacent pure chaos elements.
Type-A	Each element follows its own pure chaos dynamics with some adjustment to reduce the difference of the corresponding sensor value from the global and the local means of other sensor values.
Type-B	Each element is updated by a chaos map of its sensor value. The sensor value contains the effects of the self and the other elements mixed together through the embodiment. The mixing function does not appear explicitly in the equation. It is a non-linear and time-varying function, reflecting the physical dynamics of the body-environment interaction.
Type-C	In addition to the Type-B, some adjustment is applied in order to reduce the deviation of the corresponding sensor value from the global and the local means of other sensor values.

4 Experiments

Our model of behavior emergence is quite simple. However, its behavior is extremely complex. Even theoretically, a behavior of coupled chaotic systems with time-varying non-linear coupling is very poorly understood. Moreover, there has been no attempt so far to exploit this phenomena for robotic behavior generation. Therefore, we carried out a series of experiments in order to investigate the following points.

1. How to design the connection between the body and the chaotic elements?
2. How does the system behave in case the structure of body dynamics changes?
3. How does the system behave in case the structure of environment changes?
4. How can we impose "goal-directedness" onto the behavior while maintaining the emergent property?

In the following, we present some results from our preliminary experiments. Further details should be found in another paper [4].

We use dynamics simulation library ODE[9] to simulate the dynamics of a robot and environment. The time step size of ODE was 0.01 and that of couple chaotic system was T_c. In implementation, u and s in section 3.2 were associated with s_{raw} and m ((7), (8), (9), (10)), where s_{raw} denotes the raw value of a sensor and m the motor output of an actuator. Note that the gains $g_u, g_{u_{out}}, g_s, g_{s_{in}}$ and the offsets $o_u, o_{u_{out}}, o_s, o_{s_{in}}$ are independent of the element index i. They are constant parameters.

$$u_{out} = g_u \cdot u + o_u \tag{7}$$

$$m = g_{u_{out}} \cdot u_{out} + o_{u_{out}} \tag{8}$$

$$s_{in} = g_{s_{in}} \cdot s_{raw} + o_{s_{in}} \tag{9}$$

$$s = g_s \cdot s_{in} + o_s \tag{10}$$

4.1 Experiments with a muscle-joint model

Configuration

Firstly, we experiment with a muscle-joint model shown in Fig. 2 which consists of two cylindrical rigid bodies and 12 muscle fibers. The base link is fixed to the ground, and the upper link is connected by a ball-joint to the base link. It can be bent in any direction within the limit of 0.5 [rad]. The 12 muscle fibers are attached between the two links isotropically.

Each muscle fiber is modelled with Hill's characteristic equation [7]. m in (8) corresponds to the activation level of a muscle fiber in this model. The sensor value s_{raw} is provided by either a "length-sensor" measuring the normalized length of the muscle fiber or a "tension sensor"[3] measuring the

[3] In case of tension sensor, before the process of (10), s_{in} is constrained as follows: $if(s_{in} > 1)\ s_{in} = 1,\ if(s_{in} < -1)\ s_{in} = -1$

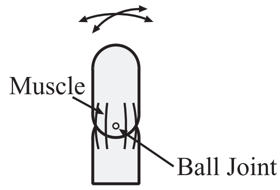

Fig. 2. Appearance of the muscle-joint model

normalized tension of the muscle fiber. In all experiments, $(g_{u_{out}}, o_{u_{out}})$ was set to $(0.5, 0.5)$ respectively. In case of tension sensor, $(g_{s_{in}}, o_{s_{in}})$ was set to $(-2.5, 3.0)$. In case of length sensor, $(g_{s_{in}}, o_{s_{in}})$ was set to $(1.0, 0.0)$.

Experiments with/without sensor feedback

Firstly, when there is no sensor feedback (Fig. 3), the motion of the joint was chaotic and no cluster structure was observed.

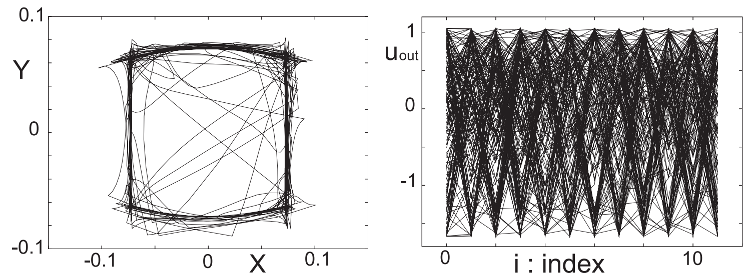

Fig. 3. Experiment with no sensor feedback. Trajectory of the center of mass of the upper link projected on $x-y$ plane (left graph). Cluster plot of the chaotic elements (right). For each element with index i, its motor output u_{out} is plotted superposedly for $n = 10, 11, 12, \ldots$. The points of all the elements are connected with a line for each time step. (Type-A, $a = 1.6$, $\varepsilon_1 = 0.0$, $\varepsilon_2 = 0.0$, $T_c = 0.21$, $g_u = 1.7$, $g_s = 2.0$, $o_u = -0.65$, $o_s = -1.0$)

Secondly, in case of an experiment with tension sensor feedback, the motion was chaotic for the initial several steps. But after a time, it changed to the ordered rhythmical motion. Fig. 4 is the graph while the motion was rhythmical. Cluster structure is observed.

In case of an experiment with length sensor feedback, the motion was ordered and rhythmical from the beginning (Fig. 5). In the same experiment with a different parameter set, the motion was rhythmical in the beginning, then after a while, the direction of oscillation changed and it began another

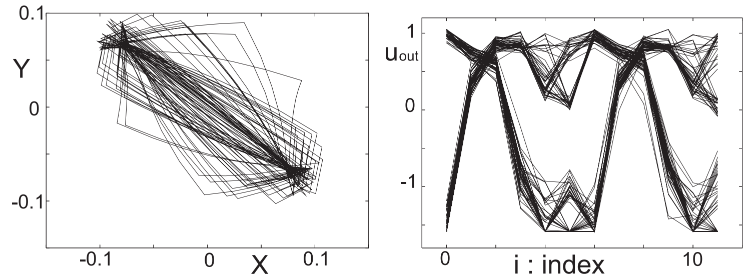

Fig. 4. Experiment with feedback of tension sensor (Type-A, tension sensor, $a = 1.55,\ \varepsilon_1 = 0.3,\ \varepsilon_2 = 0.3,\ T_c = 0.21,\ g_u = 1.7,\ g_s = 2.0,\ o_u = -0.65,\ o_s = -1.0$)

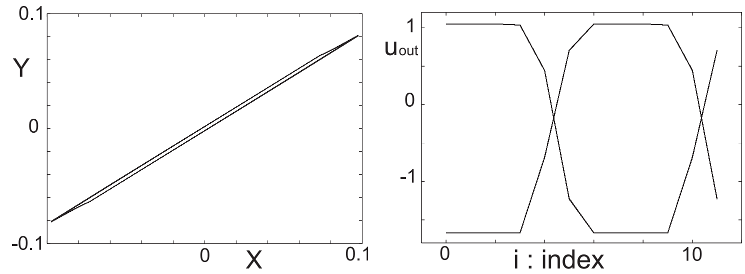

Fig. 5. Experiment with feedback of length sensor (Type-B, length sensor, $a = 1.6,\ T_c = 0.21,\ g_u = 1.7,\ g_s = 1.0,\ o_u = -0.65,\ o_s = 0.0$)

rhythmical motion (Fig. 6). The change of oscillating direction occurred aperiodically.

Experiments with a dynamic change of the environmental structure

The environment makes a part of the interaction field for the chaotic elements. In this experiment, we observed the system's behavior when the structure of the environment is dynamically changed by bringing in an obstacle disturbing the oscillation of the muscle-joint system (Fig. 7).

The obstacle was brought in at $t = 3$. Fig. 8 shows the result : beginning at the top, from $t = 0.42$ to $t = 3.15$, from $t = 3.15$ to $t = 6.93$, and from $t = 6.93$ to $t = 12.6$. A little while after colliding against the obstacle, the joint made a complex motion that it repeated colliding in a short period of time and the motor commands were chaotic. But soon after that, within about 3 seconds, it began to oscillate orderly in a new collision-free direction.

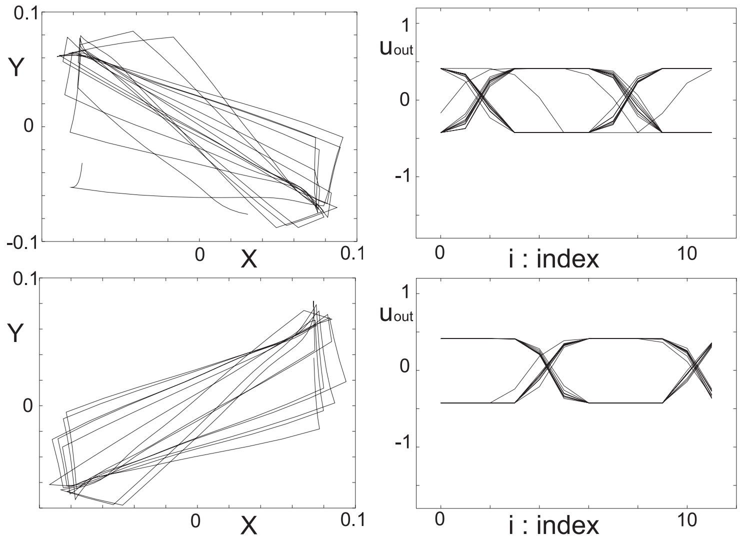

Fig. 6. Experiment when dynamic transitions could be seen. The upper graph shows the behavior before transition and the lower one shows that after transition. (Type-A, length sensor, $a = 1.6,\ T_c = 0.21,\ g_u = 0.52,\ g_s = 1.0,\ o_u = -0.107,\ o_s = 0.0$)

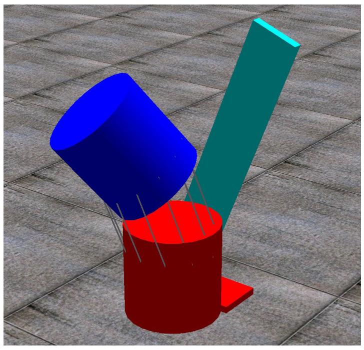

Fig. 7. The muscle joint model and obstacle

4.2 Experiments with an insect-like multi-legged robot

Configuration

In order to investigate the effects of our model in a more meaningful behavior with more complex interactions with the environment, we defined an insect-like multi-legged robot. The robot has a disc-shaped body with 12 legs attached on its fringe with regular spacing (Fig. 9). Each leg is connected to the body by a rotational joint and 2 springs whose spring constant is K. Each

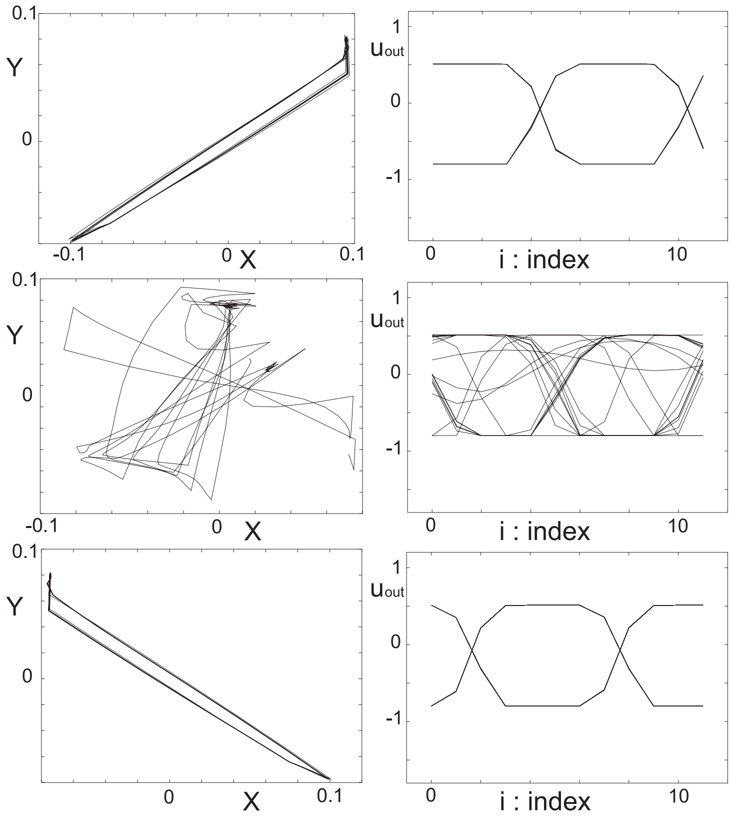

Fig. 8. Experiment with obstacle (Type-B, length sensor, $a = 1.6,\ T_c = 0.21,\ g_u = 0.82,\ g_s = 1.0,\ o_u = -0.3,\ o_s = 0.0$)

leg can swing only in the direction shown in the middle of Fig. 9, and its joint angle is constrained to be less than $\pm\theta_{lim}$. The environment has a standard gravity and a constant friction (with the static friction coefficient μ). m in (8) corresponds to the torque τ of each joint. s_{raw} in (9) corresponds to the angle θ. Table 2 shows the parameters common to all the experiments using the above robot model.

Table 2. Parameters for the insect-like robot

T_c	K	θ_{lim}	$g_{u_{out}}$	g_s	$g_{s_{in}}$	$o_{u_{out}}$	o_s	$o_{s_{in}}$
0.17	1.0	0.8	1.0	0.5	1.25	0.0	0.5	0.0

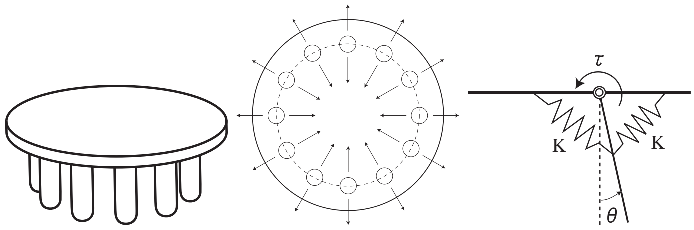

Fig. 9. Appearance of the insect-like robot (left), direction of leg motion(middle), and the mechanism of a leg (right).

Experiments with sensor feedback

With no sensor feedback, no order was observed in the motion of the robot. It just kept on randomly struggling around the same spot on the ground.

On the other hand, when the sensor feedback is introduced, after the initial chaotic period (a few seconds), the robot started to move in a certain direction, and then finally showed a stable locomotive behavior with a constant speed in a stable direction. The locomotive behavior was realized by synchronizing the 3 or 4 hind legs and kicking the ground with them. Fig. 10 is the graph while the locomotive behavior was observed.

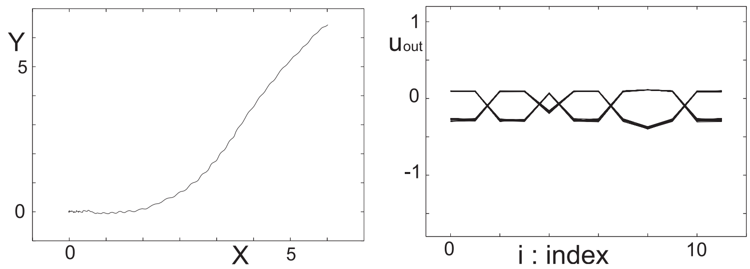

Fig. 10. Experiment with sensor feedback (Type-C, $a = 1.47$, $\varepsilon_1 = 0.1$, $\varepsilon_2 = 0.1$, $g_u = 0.4$, $o_u = -0.28$, $\mu = 0.1$)

4.3 Summary

The proposed model exhibited a capability to quickly discover various motion patterns in accordance with the body-environment dynamics. It can cope with dynamically changing constraints. In other experiments [4], we confirmed that the model can adapt to changes of the muscle arrangements, the capability persists over a range of parameters, and a possibility of imposing goal-directedness on the emergent behavior.

5 Simulated Baby

The above model correlates with the essential structure of vertebrates, i.e. the spine/medulla circuit and the musculo-skeletal body. It is well established that parts of spine/medulla circuit acts as non-linear oscillators, called CPG (central pattern generator). Under certain conditions, a coupled system of non-linear oscillators act as a coupled chaotic system. Therefore, it is quite plausible that vertebrates exploit the similar principle as our model for acquisition and adaptation of motor behavior.

Since our model explores and discovers motion patterns that fit the natural property of the body, it may be a good candidate for simulating the initial mechanism of motor development. It may be able to start with very little predefined knowledge and autonomously acquire appropriate motor primitives.

A human body is so complex, and a systematic search for all possible motion patterns is virtually impossible. However, our model should be able to discover appropriate motions very quickly. Moreover, the cluster emergence in pure CML and GCM are known to scale to thousands of elements. This is a good reason to expect that our model can handle the musculo-skeletal system of a human body.

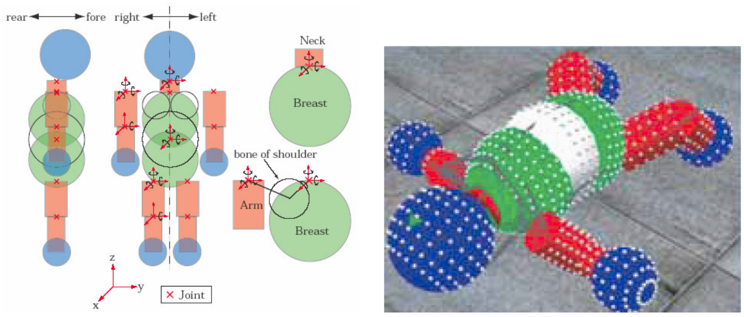

Fig. 11. Simulated baby.

Figure 11 shows the view of our simulated baby. The outlook is crude as we invest little effort on the quality of graphics. However, the musculo-skeletal system is modeled at a highly detailed level. Our model has 198 muscles. We omitted the wrist, ankle, fingers, toes, neck and face. But the body stem and the limbs are quite faithfully modeled. The dimensions, mass, and inertial parameters of all the body parts are defined according to the measurements of real babies. The proprioceptive sensing organs, i.e. the muscle spindles and Golgi tendon organs, are also modeled as precisely as possible. The muscles are also modeled to match the performance of real babies. All the physical body parameters are modeled as functions of week age after gestation (in the uterus). So the body can simulate physical growth of the fetal and neonatal periods.

As the first step of neural modeling, we adopted the same coupled chaos model (in section 4) for the spinal circuit. In addition, we added self-organizing maps to simulate sensory and motor areas of the cerebral cortex. All the connections are continuously updated by Hebbian learning while the neural system drives the body.

The simulated baby body is placed in two types of simulated environments; The "fetus" is placed in a simulated uterus with a pushable wall, filled with liquid. The "neonate" is placed on a flat floor surrounded by flat walls (like a playpen). We are starting to observe emergence of patterned motions and stable clustering of cortical neurons.

6 Summary and Discussions

We proposed a novel framework for highly (quick) adaptive motor behavior. The core mechanism is based on coupled chaotic system, which autonomously explores and generates various coordination patterns of multiple degrees of freedom. The emergent motion patterns exploit and resonate with the body-environment dynamics. Therefore our model is a very good candidate as the initial core mechanism to simulate very early motor development of human babies. It should be important for human babies to acquire motor primitives exploiting the characteristics of body-environment dynamics.

The above model correlates with real human babies because the CPG in spine/medulla can generate high dimensional chaos under certain conditions, and the resulting whole body movement has the similar property as the general movement (GM) which appears in early motor development of human babies.

We are now constructing and experimenting with a simulated baby. It is designed to be very close to real human babies in terms of musculo-skeletal system. The coupled chaotic system model is adopted as the basic mechanism of behavior emergence. When an emergent motion pattern persists for certain time duration, the learning in the cortex model and other neural connections fixates it in the neural connections. This way the system should be able to explore, discover and learn various motor primitives which fully exploit the natural body-environment dynamics. It is still an open question how to design a mechanism that appropriately integrate the learning and emergence.

The above approach may provide a solution to avoid the frame problem, as the system does not rely on static (or very slowly adapting) internal representations, and can immediately adapt to changing situations.

Acknowledgement

This work was partially supported by Grant-in-Aid for Scientific Research from JSPS, Japan, and JST ERATO Asada Project. The authors would like to express their thanks to Prof. Ichiro Tsuda, Prof. Rolf Pfeifer, Porf. Kazuyuki Aihara, Prof. Minoru Asada and many other researchers for the valuable discussions.

References

1. R. R. Burridge, A. A. Rizzi, and D. E. Koditschek. Sequential composition of dynamically dexterous robot behaviors. *Int. J. Robotics Research*, 18(6):534–555, 1999.
2. K. Kaneko and I. Tsuda. *Complex Systems: Chaos and Beyond.* Springer, 2001.
3. Y. Kuniyoshi, Y. Ohmura, K. Terada, and A. Nagakubo. Dynamic roll-and-rise motion by an adult-size humanoid robot. *Int. J. of Humanoid Robotics*, 1(3):497–516, 2004.
4. Y. Kuniyoshi and S. Suzuki. Dynamic emergence and adaptation of behavior through embodiment as coupled chaotic field. In *Proc. IEEE Int. Conf. on Intelligent Robots and Systems*, pages 2042–2049, 2004.
5. T. McGeer. Passive dynamic walking. *Int. J. of Robotics Research*, 9(2), 1990.
6. Zenon W. Pylyshyn. *The Robot's Dilemma: The Frame Problem in Artificial Intelligence.* Ablex, 1987.
7. Nakamura R. and Saito H. *Kisoundougaku.* Ishiyakushuppan, 4 edition, 1992.
8. A. A. Rizzi and D. E. Koditschek. Further progress in robot juggling: The spatial two-juggle. In *Proc. IEEE Int. Conf. Robotics and Automation*, pages 919–924, 1993.
9. Russell Smith. Open dynamics engine(ode). http://opende.sourceforge.net/ode.html.
10. G. Taga, Y. Yamaguchi, and H. Shimizu. Self-organized control of bipedal locomotion by neural oscillators in unpredictable environment. *Biological Cybernetics*, 65:147–159, 1991.